Progress In Electromagnetics Research C, Vol. 73, 167–176, 2017

Dual-Band Omnidirectional Circularly Polarized Patch Antenna with Etched Slots and Shorting Vias

Hong-Yin Zhang*, Fu-Shun Zhang, Can Wang, and Tian Li

Abstract—A dual-band omnidirectional circularly polarized (CP) patch antenna with conical radiation patterns is presented in this paper. The antenna consists of a patch with inclined slots, a ground plane with L-shaped slots and a coaxial probe. In addition, by loading shorting vias between the patch and the ground plane, the vertical polarizations of the proposed antenna at TM_{01} and TM_{02} modes can be obtained. Two sets of slots etched on the ground and the patch contribute to the horizontal polarizations for the two modes, respectively. Omnidirectional CP fields can be achieved at both resonant modes when the two orthogonal polarizations are equal in amplitude and different in phase by 90°. To verify the design, a prototype operating at 2.4 GHz WLAN and 3.5 GHz WiMAX bands has been fabricated and measured. The measured average axial ratios (ARs) at two resonant modes in the azimuth plane are 1.1 and 1.5 dB, respectively. Experimental results show good agreement with the simulated data.

1. INTRODUCTION

Omnidirectional circularly polarized (CP) antennas can not only alleviate the multipath interference and polarization mismatch between the receiving and transmitting antennas, but also serve 360° full coverage. Due to their outstanding advantages, a lot of efforts have been put into designing omnidirectional CP antennas over the past few years. In the designs of [1–4], the fed dipole/coaxial probe and loop/bended branches are utilized to generate vertically and horizontally polarized omnidirectional fields, respectively. Differently, each of the array elements in [5, 6] is firstly designed to be a CP antenna. Then these CP array elements are arranged in a circular/square formation to achieve omnidirectional radiation. In addition, the omnidirectional CP properties can be realized by dielectric resonator antennas (DRA) [7–9]. In general, the DRA fed centrally by a coaxial probe could offer a vertical polarization in these designs. And then several inclined slits are fabricated on the sidewalls of the DRA to achieve omnidirectional CP fields. Recently, many antennas with low profiles using higher-order modes are also proposed to achieve good omnidirectional CP performances [10–13].

However, relatively few designs of dual-frequency CP antennas with omnidirectional radiation patterns have been reported [14–17]. In [14], a dual-frequency omnidirectional right hand CP (RHCP) antenna is achieved by employing back-to-back coupled patches. However, the proposed structure is not low in profile. The antennas in [15, 16] utilize coaxial probes and Alford loops to achieve omnidirectional dual-band dual-sense CP properties. However, compared to these designs with expanding stubs, the proposed structure in [17] has a great size reduction. Additionally, the antenna in [17] using TM_{01} and TM_{02} modes can also provide good radiation properties. It should be noted that the antenna is realized at the expense of complex slot structures.

In this paper, the proposed antenna is composed of a square-ring patch, a modified ground plane, and a set of shorting vias which connect the patch and ground plane. The TM_{01} mode introduced

Received 14 February 2017, Accepted 12 April 2017, Scheduled 24 April 2017

* Corresponding author: Hong-Yin Zhang (honyin0701@163.com).

The authors are with the National Key Laboratory of Antennas and Microwave Technology, Xidian University, Xi'an 710071, P. R. China.

by the shorting vias and the basic TM_{02} mode of the monopolar patch antenna are responsible for the vertical polarizations. And the horizontal polarizations at two resonant modes can be obtained by etching four inclined slots and four L-shaped slots on the patch and ground. Therefore, a CP radiation can be formed when two orthogonal polarizations are equal in amplitude and quadrature in phase. In addition, the upper and lower frequency bands can be tuned by changing the dimensions of the patch and ground separately. And the CP senses of the proposed design can also be changed by reconfiguring the directions of slots on the patch and ground, respectively. Such features are desirable as they greatly simplify the design process.

2. ANTENNA CONFIGURATION

Figure 1 shows the configuration of the proposed dual-band omnidirectional CP antenna. The antenna can be divided into four parts, namely a square-ring patch with four inclined slots, a square ground plane with four L-shaped slots, four shorting vias and a coaxial probe. As shown in Figure 1(a), the square-ring patch, having an outer side length of $L1$ and inner side length of $C2$, and the inner square patch, having a side length of $C1$, are etched on the same side of an FR4 substrate (thickness 2 mm, permittivity 4.4). Meanwhile, four inclined slots are introduced on the patch. And the ground with four sequentially-rotated L-shaped slots is etched on substrate 2 whose thickness and relative dielectric constant are 2 mm and 2.65, respectively. There is an air layer between two different substrates, and its thickness is 2.5 mm. In this design, four shorting vias with radius $R1$ are introduced to generate TM_{01} mode of the vertical polarizations for the proposed antenna. In addition, for providing symmetrical radiation pattern performances across both bands, the antenna is fed by a coaxial probe of radius 0.6 mm through gap coupling at the center of the substrate.

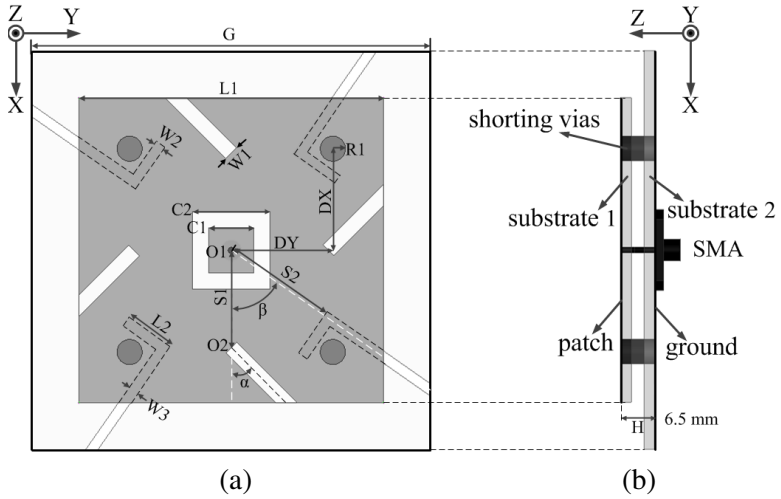

Figure 1. Configuration of the proposed antenna. (a) Front view; (b) side view.

3. ANTENNA DESIGN

The proposed antenna, based on its vertical polarizations and horizontal polarizations, is able to provide a dual-band omnidirectional CP property. The vertical polarizations are provided by the top-loaded monopolar patch antenna, which has two resonant modes, namely TM_{01} and TM_{02} modes [18, 19]. The TM_{01} mode is introduced by the shorting vias and has a similar property of the lowest mode in the monopolar wire-patch antennas discussed in [18]. For the TM_{02} mode, it is a perturbed mode of TM_{02} mode in the patch antenna without wire shorted [19]. To distinguish each resonant mode, Figure 2 plots the electric fields of the cavity model for the proposed antenna at two frequencies, namely 2.45 GHz and 3.5 GHz. It can be seen that the electric fields for the two modes are similar, except one significant

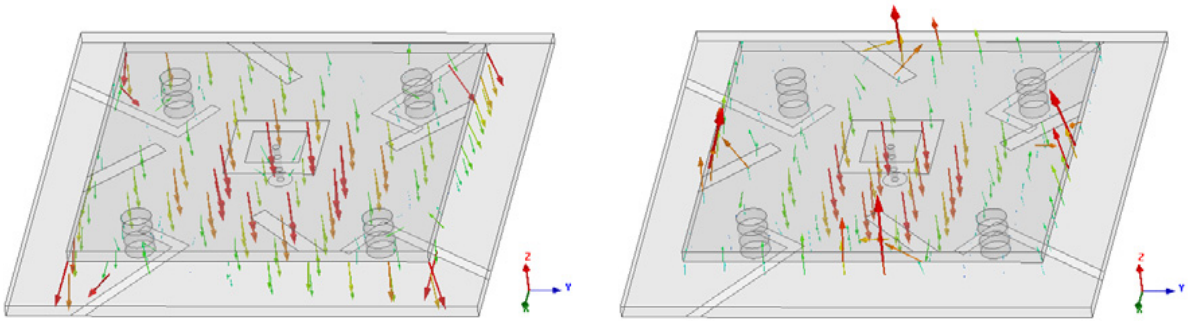

Figure 2. (a) Electric fields for TM_{01} mode of the cavity model at 2.45 GHz; (b) Electric fields for TM_{02} mode of the cavity model at 3.5 GHz.

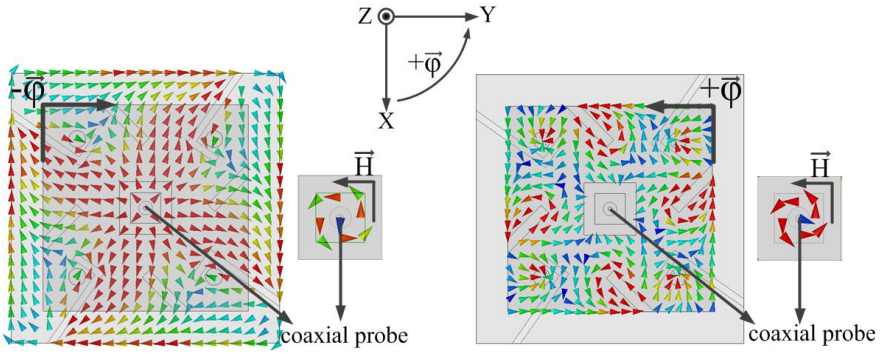

Figure 3. (left) Currents distributions on the ground/patch and (right) magnetic fields distributions around the coaxial probe. (a) TM_{01} mode; (b) TM_{02} mode.

difference that the electric fields for the TM_{01} mode have the same directions at the inside/outside of four shorting vias, while the electric fields for the TM_{02} mode have opposite directions. In addition, the horizontal polarizations at two resonant modes can be obtained by etching four inclined slots and four L-shaped slots on the patch and ground. And the magnitude ratio and phase difference for two orthogonal polarizations at two modes can be tuned by changing the dimensions of the shorting vias and slots. Thus, a CP radiation can be formed when the vertical and horizontal polarizations are equal in amplitude and quadrature in phase.

To better understand the operating principle, Figure 3 demonstrates the surface currents distributed on the ground/patch and the magnetic fields distributed around the coaxial probe. With reference to Figure 3, the surface currents in the direction of Z and φ could provide vertical and horizontal polarizations (E_θ and E_φ), respectively. For the TM_{01} mode, the vertically polarized fields E_θ are provided by the currents on the coaxial probe. It can be seen from Figure 3(a)(right) that the magnetic fields around the coaxial probe are in the counter-clockwise direction. According to the boundary condition ($\overrightarrow{J} = \widehat{n} \times \overrightarrow{H}$), the currents on the coaxial probe, in the direction of $+Z$, can be concluded here. In addition, the horizontally polarized fields E_φ are dominated by the currents in the $-\varphi$ direction flowing along the slots on the ground, as shown in Figure 3(a)(left). For the TM_{02} mode, as shown in Figure 3(b)(right), the currents on the coaxial probe in the direction of $+Z$ dominate the vertical polarization E_θ. Differently, the horizontal polarization E_φ is provided by the currents in the $+\varphi$ direction distributed on the patch, which can be validated in Figure 3(b)(left). Thus, it can be concluded that the proposed antenna can radiate dual-sense CP waves at two resonant modes because of the inverse direction for the horizontal polarization E_φ. In addition, by carefully tuning the dimensional parameters, a balance between the horizontal and vertical polarizations can be achieved, which facilities obtaining good omnidirectional CP properties. Finally, the detailed geometry and dimensions of the proposed antenna are given in Figure 1 and Table 1 after optimization with ANSYS HFSS.

Table 1. Dimensions of the proposed antenna.

Parameter	Value	Parameter	Value	Parameter	Value
G	78.8 mm	$W3$	2.0 mm	$R1$	2.5 mm
$L1$	60.2 mm	$C1$	9.0 mm	$S1$	19.2 mm
$L2$	10.0 mm	$C2$	15.3 mm	$S2$	22.5 mm
$W1$	3.0 mm	DX	20.1 mm	α	45 deg
$W2$	2.0 mm	DY	20.1 mm	β	55 deg

4. PARAMETRIC STUDY

To characterize the proposed dual-band omnidirectional CP antenna, a parametric study is carried out in this section. And the effects of vital parameters, such as G, $L1$, $R1$, DX and H, on the resonant frequency and axial ratio (AR) are discussed. In addition, all the other parameters not mentioned stay constant as shown in Table 1 during this process.

4.1. Effect of the Variation of the Ground and L-Shaped Slot Size

First, the effect of the ground dimension on the antenna performance is studied. Figure 4 depicts the simulated reflection coefficient and AR of the proposed antenna with different ground dimensions G. It should be noted that the variation of the ground implies the variation of four L-shaped slots on the ground for this antenna. It can be seen from Figure 4(a) that, as G increases, the lower resonant frequency shifts downward, while the upper resonant frequency stays almost the same. Actually, it can be expected that a longer L-shaped slot (namely a larger ground) should have a lower resonant frequency. In addition, the horizontal polarizations of the antenna at the TM_{01} mode is generated by four L-shaped slots on the ground. Therefore, the AR has a similar trend to the reflection coefficient at this mode, which can be validated in Figure 4(b).

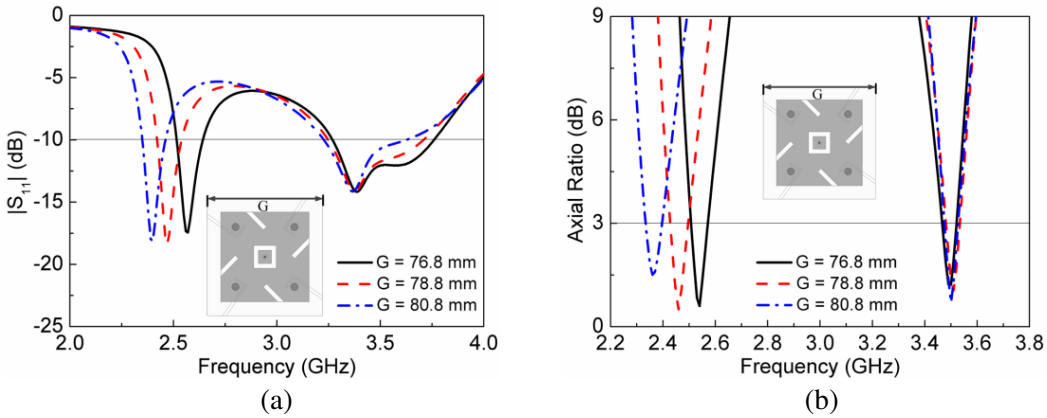

(a) (b)

Figure 4. Simulated reflection coefficient and AR of the dual-band omnidirectional CP antenna for different $G = 76.8$, 78.8 and 80.8 mm. (a) Reflection coefficient; (b) AR.

4.2. Effect of the Variation of the Patch and Inclined Slot Size

The effect of the patch dimension is studied next. Figure 5 demonstrates the simulated reflection coefficient and AR of the proposed antenna with different patch dimensions $L1$. Here, the variation of the patch implies the variation of the four inclined slots on the patch for this antenna. With reference to Figure 5, it can be seen that the TM_{02} modes for reflection coefficient and AR shift upward as $L1$ decreases, while the TM_{01} modes of the proposed antenna keep almost unchanged. It can be concluded

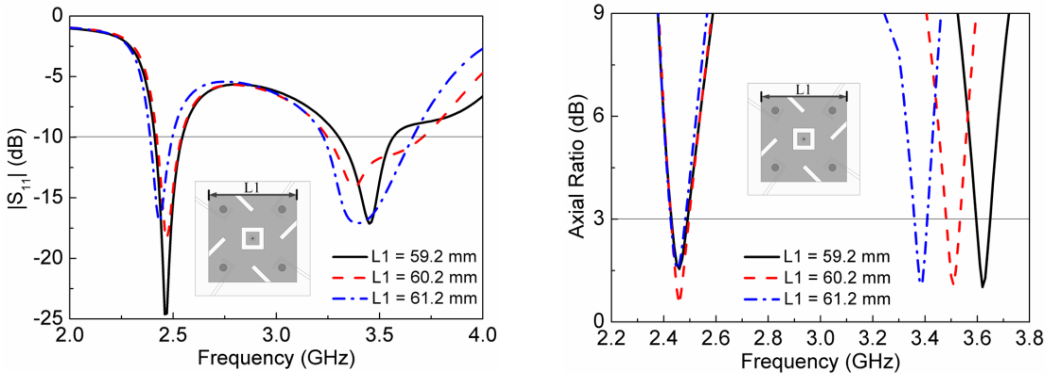

Figure 5. Simulated reflection coefficient and AR of the dual-band omnidirectional CP antenna for different $L1 = 59.2$, 60.2 and 61.2 mm. (a) Reflection coefficient; (b) AR.

that the lengths of four inclined slots on the patch have a critical effect on the TM_{02} modes for reflection coefficient and AR. It should be mentioned that both the reflection coefficient and AR are tightly related to G and $L1$ at two resonant frequencies. To obtain two given frequencies, the sizes of the ground and patch can be adjusted independently.

4.3. Effect of the Variation of the Shorting Vias $R1$

The effect of shorting vias on the simulated reflection coefficient and AR of the proposed antenna is also investigated. As shown in Figure 6, it can be seen that radius $R1$ of shorting vias has a greater effect on the lower resonant frequency than upper resonant frequency for the reflection coefficient and AR. This is because the new TM_{01} mode in the lower frequency band is created by loading shorting vias. In addition, by tuning $R1$ carefully, good CP properties can be achieved across two operating bands.

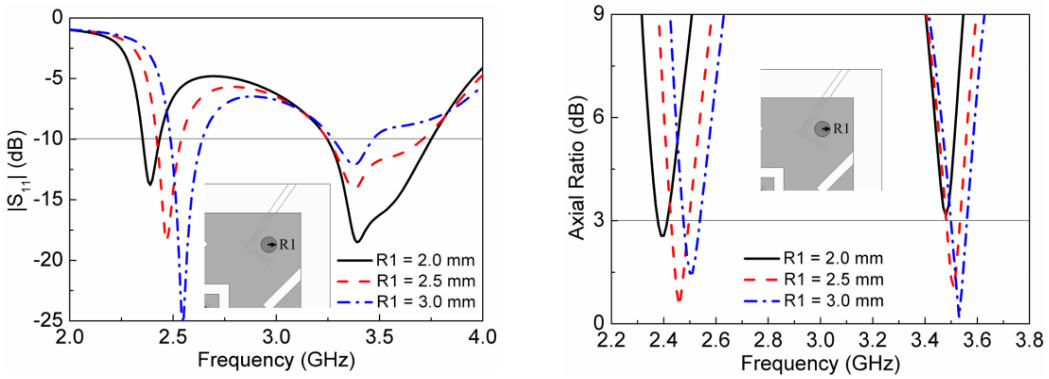

Figure 6. Simulated reflection coefficient and AR of the dual-band omnidirectional CP antenna for different $R1 = 2.0$, 2.5 and 3.0 mm. (a) Reflection coefficient; (b) AR.

4.4. Effect of the Variation of the Distance DX

Figure 7 shows the simulated reflection coefficient and AR for different positions (DX) of shorting vias. The variations of reflection coefficient and AR with DX are similar to those of $R1$, and therefore, they are not shown in detail here. In addition, the CP properties may get worse when the parameter DX changes at both modes. The reason can be that the respective polarization purity of the two orthogonal

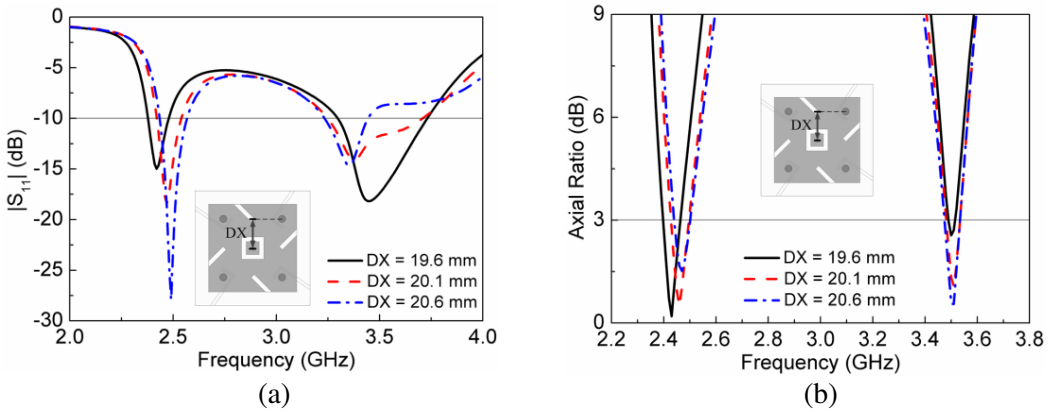

(a) (b)

Figure 7. Simulated reflection coefficient and AR of the dual-band omnidirectional CP antenna for different $DX = 19.6$, 20.1 and 20.6 mm. (a) Reflection coefficient; (b) AR.

modes gets deteriorated with the variation of position DX. Finally, two vital parameters ($R1$ and DX) are selected as 2.5 mm and 20.1 mm to obtain relatively better dual-band omnidirectional CP properties.

4.5. Effect of the Variation of the Antenna Height H

Finally, the effect of the antenna height H is investigated. As shown in Figure 8(a), the input impedance at the TM_{02} mode is strongly affected by H. As we know, the variation of the height H can change the equivalent dielectric constant of the antenna. This may be the reason that the TM_{02} mode highly depends on the antenna height. With reference to Figure 8(b), AR remains unchanged as H varies. It suggests that the impedance matching at the TM_{02} mode can be accomplished by adjusting H without affecting AR.

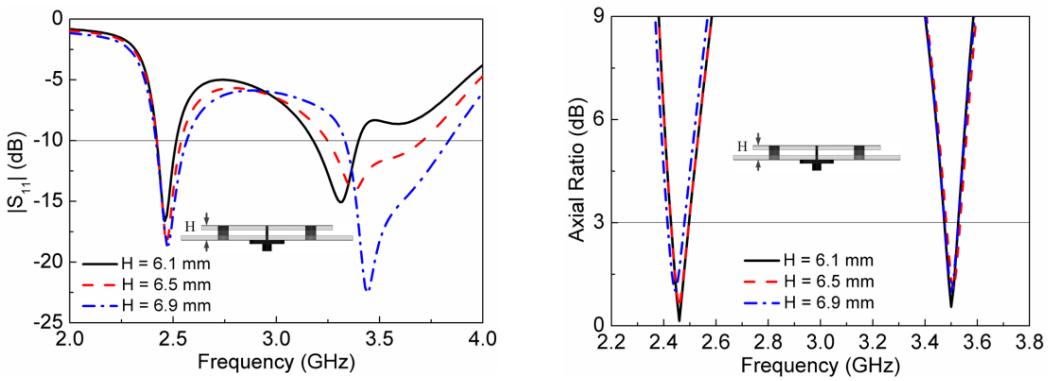

(a) (b)

Figure 8. Simulated reflection coefficient and AR of the dual-band omnidirectional CP antenna for different $H = 6.1$, 6.5 and 6.9 mm. (a) Reflection coefficient; (b) AR.

In summary, the ground and patch dimensions (G and $L1$) have great effects on both the input impedance and AR at the TM_{01} and TM_{02} modes, respectively. By adjusting the parameters (G and $L1$) carefully, the frequency ratio of the two resonant modes can be tuned. Additionally, the shorting vias dimensions ($R1$ and DX) mainly affect the reflection coefficient and AR at the TM_{01} mode, while the antenna height (H) affects the input impedance at the TM_{02} mode only. Therefore, properties of these vital parameters can be used to greatly simplify the design process.

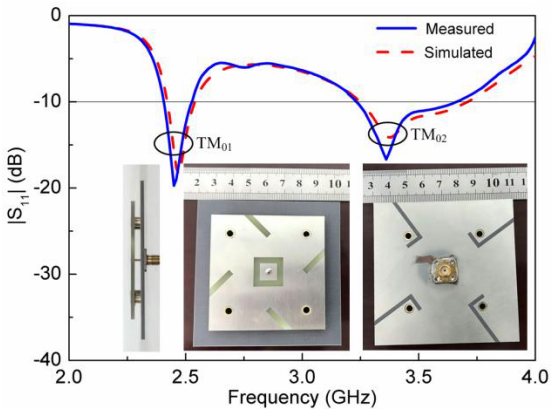

Figure 9. Simulated and measured $|S_{11}|$ and the photographs of the fabricated antenna.

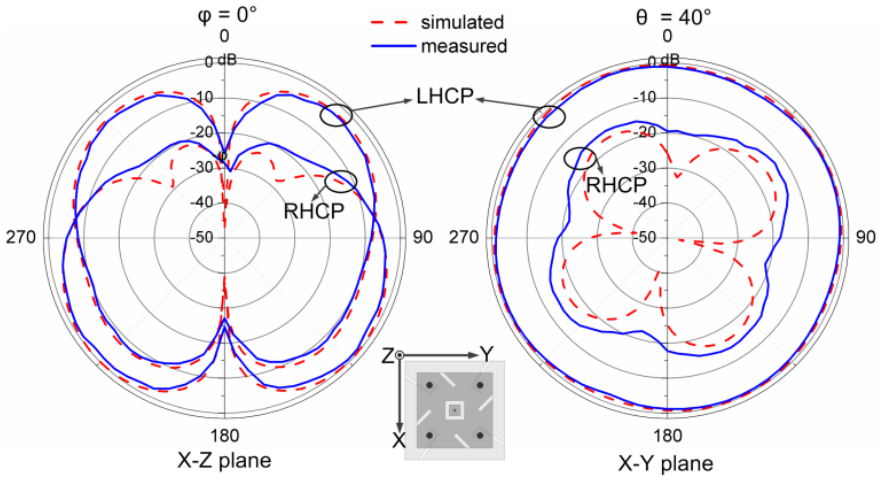

(a)

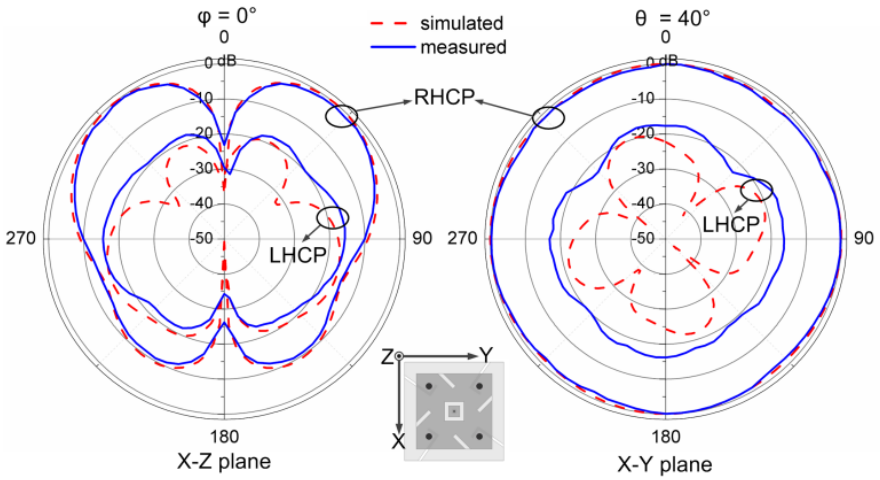

(b)

Figure 10. Simulated and measured radiation patterns in the elevation ($\varphi = 0°$) and azimuth ($\theta = 40°$) planes. (a) 2.45 GHz; (b) 3.5 GHz.

5. SIMULATED AND MEASURED RESULTS

To verify the design, a prototype of the proposed antenna has been fabricated and measured. Measurements on the impedance bandwidth are accomplished by the Wiltron 37269A Network Analyzer, and the gains and radiation patterns are measured by the time-gating method. The simulated and measured $|S_{11}|$ are depicted in Figure 9, and good agreement between them is obtained. With reference to the Figure 9, it is clearly observed that two resonant modes (TM_{01} and TM_{02}) are excited, and the measured 10-dB impedance bandwidths ($|S_{11}| < -10\,\text{dB}$) in the lower and upper bands are 5.3% (2.4–2.53 GHz) and 13.6% (3.23–3.7 GHz), respectively. Therefore, the proposed antenna can provide operating bands covering 2.4 GHz WLAN and 3.5 GHz WiMAX successfully.

Figure 10 shows the simulated and measured radiation patterns in the elevation ($\varphi = 0°$) and azimuth ($\theta = 40°$) planes at 2.45 GHz and 3.5 GHz. It can be seen that the proposed antenna radiates LHCP and RHCP waves in the half space of $+Z$ axis at two resonant frequencies, respectively. It should be noted that the maximum directions occur in different directions for the X-Z plane patterns at two resonant frequencies. For the upper frequency, with the ground as a reflector, its maximum directions occur at $\theta = 40°$. Because L-shaped slots are etched on the ground, the radiation fields at the lower frequency are bidirectional. In addition, the elevation patterns at two resonant modes have a null in the boresight direction ($\theta = 0°$) whereas the azimuthal patterns are omnidirectional. And the

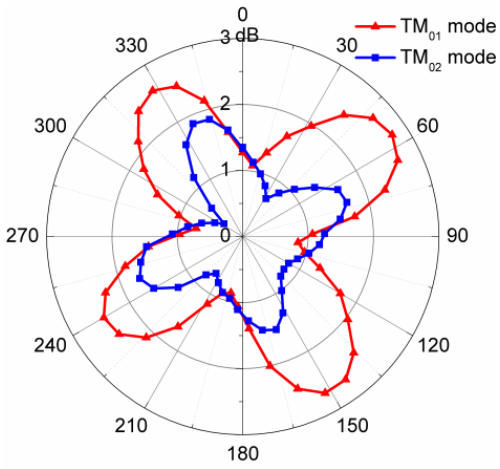

Figure 11. Measured ARs in the azimuth ($\theta = 40°$) planes.

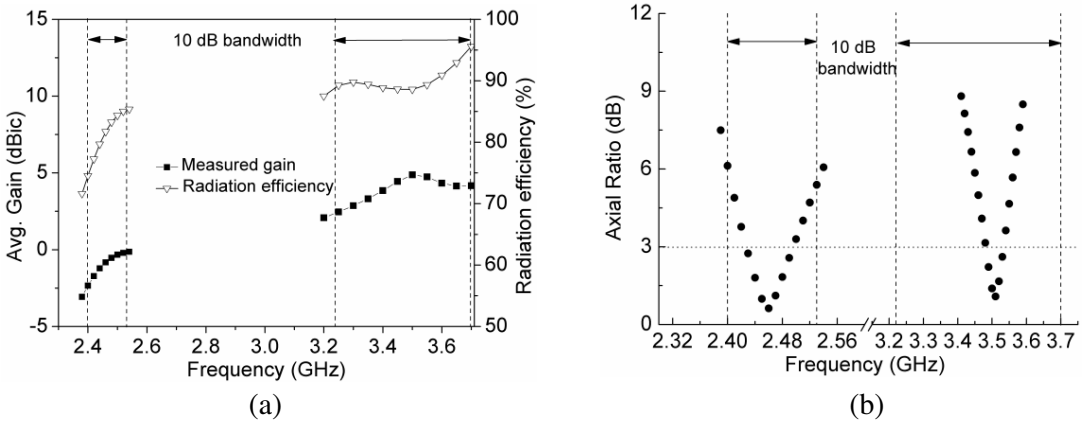

Figure 12. (a) Measured average gain versus frequency (at $\theta = 40°$); (b) measured AR versus frequency (at $\theta = 40°$, $\varphi = 0°$).

co-polarization levels are both at least 16 dB stronger than the cross-polarizations for whole azimuth planes. To better understand the omnidirectional CP property, the AR patterns with different φ at $\theta = 40^\circ$ at two resonant frequencies are provided in Figure 11. It can be seen that the measured ARs at both resonant modes in the azimuth planes are less than 3 dB, proving the good omnidirectional CP property of the proposed antenna.

Finally, the measured gains, radiation efficiencies and ARs across two operating bands are shown in Figure 12. In Figure 12(a), the measured average LHCP and RHCP gains from -2.3 to -0.1 and 2.1 to 4.2 dBic at $\theta = 40^\circ$ in the lower and upper bands are obtained, respectively. The measured efficiencies of 74.5%–85% and 88.6%–95.6% are obtained over two bands, respectively. Figure 12(b) shows the measured ARs of the prototype in the direction of $\theta = 40^\circ$ and $\varphi = 0^\circ$. The measured ARs at two center frequencies are about 0.6 and 1.1 dB, respectively. In addition, the ARs in the azimuth plane are also measured and all less than 3 dB, proving the good omnidirectional CP property of the prototype.

6. CONCLUSION

A dual-band omnidirectional CP patch antenna has been investigated and fabricated in this paper. With a low profile of $0.052\lambda_0$ (λ_0 is the free space wavelength at 2.4 GHz), the antenna can achieve good omnidirectional CP properties at two resonant modes. And two frequency bands can be independently controlled by the dimensions of ground plane and patch, respectively, which can greatly simplify the design process. In addition, the measured results show that the antenna can operate at 2.4 WLAN and 3.5 WiMAX, which agree well with the simulated results. The measured LHCP and RHCP gains at two center frequencies in the azimuth plane are -0.8 and 4.9 dBic, respectively. The proposed antenna is suitable for the applications of the present wireless communications.

ACKNOWLEDGMENT

This work was supported by the National Natural Science Foundation of China (NSFC) under Grants No. 51405364.

REFERENCES

1. Yu, Y. F., Z. X. Shen, and S. L. He, "Compact omnidirectional antenna of circular polarization," *IEEE Antennas Wireless Propag. Lett.*, Vol. 11, 1466–1469, 2012.
2. Li, B., S. W. Liao, and Q. Xue, "Omnidirectional circularly polarized antenna combining monopole and loop radiators," *IEEE Antennas Wireless Propag. Lett.*, Vol. 12, 607–610, 2013.
3. Liu, Y., J. X. Wang, L. Yang, Y. Liu, X. Li, and J. Ren, "A compact omni-directional circularly polarized antenna for WLAN applications," *Microwave Opt. Technol. Lett.*, Vol. 58, No. 5, 1011–1016, May 2016.
4. Shi, J., X. Wu, X. M. Qing, and Z. N. Chen, "An omnidirectional circularly polarized antenna array," *IEEE Trans. Antennas Propag.*, Vol. 64, No. 2, 574–581, Feb. 2016.
5. Lau, K. L. and K. M. Luk, "A wideband circularly polarized conical-beam patch antenna," *IEEE Trans. Antennas Propag.*, Vol. 54, No. 5, 1591–1594, May 2006.
6. Quan, X. L., R. L. Li, and M. M. Tentzeris, "A broadband omnidirectional circularly polarized antenna," *IEEE Trans. Antennas Propag.*, Vol. 61, No. 5, 2363–2370, May 2013.
7. Pan, Y. M., K. W. Leung, and K. Lu, "Omnidirectional linearly and circularly polarized rectangular dielectric resonator antennas," *IEEE Trans. Antennas Propag.*, Vol. 60, No. 2, 751–759, Feb. 2012.
8. Pan, Y. M. and K. W. Leung, "Wideband omnidirectional circularly polarized dielectric resonator antenna with parasitic strips," *IEEE Trans. Antennas Propag.*, Vol. 60, No. 6, 2992–2997, Jun. 2012.
9. Khalily, M., M. R. Kamarudin, M. Mokayef, and M. H. Jamaluddin, "Omnidirectional circularly polarized dielectric resonator antenna for 5.2-GHz WLAN applications," *IEEE Antennas Wireless Propag. Lett.*, Vol. 13, 443–446, 2014.

10. Pan, Y. M., S. Y. Zheng, and B. J. Hu, "Wideband and low-profile omnidirectional circularly polarized patch antenna," *IEEE Trans. Antennas Propag.*, Vol. 62, No. 8, 4347–4351, Aug. 2014.
11. Yu, D., S. X. Gong, Y. T. Wan, Y. L. Yao, Y. X. Xu, and F. W. Wang, "Wideband omnidirectional circularly polarized patch antenna based on vortex slots and shorting vias," *IEEE Trans. Antennas Propag.*, Vol. 62, No. 8, 3970–3977, Aug. 2014.
12. Shi, Y. Z. and J. H. Liu, "Wideband and low-profile omnidirectional circularly polarized antenna with slits and shorting-vias," *IEEE Antennas Wireless Propag. Lett.*, Vol. 15, 686–689, 2016.
13. Cai, Y. M., S. Gao, Y. Z. Yin, W. T. Li, and Q. Luo, "Compact-size low-profile wideband circularly polarized omnidirectional patch antenna with reconfigurable polarizations," *IEEE Trans. Antennas Propag.*, Vol. 64, No. 5, 2016–2021, May 2016.
14. Narbudowicz, A., X. L. Bao, and M. J. Ammann, "Dual-band omnidirectional circularly polarized antenna," *IEEE Trans. Antennas Propag.*, Vol. 61, No. 1, 77–83, Jan. 2013.
15. Park, B. C. and J. H. Lee, "Dual-band omnidirectional circularly polarized antenna using zeroth- and first-order modes," *IEEE Antennas Wireless Propag. Lett.*, Vol. 11, 407–410, 2012.
16. Pan, Y. M., S. Y. Zheng, and W. W. Li, "Dual-band and dual-sense omnidirectional circularly polarized antenna," *IEEE Antennas Wireless Propag. Lett.*, Vol. 13, 706–709, 2014.
17. Yu, D., S. X. Gong, Y. T. Wan, and W. F. Chen, "Omnidirectional dual-band dual circularly polarized microstrip antenna using TM_{01} and TM_{02} modes," *IEEE Antennas Wireless Propag. Lett.*, Vol. 13, 1104–1107, 2014.
18. Jecko, B. and C. Decroze, "The 'monopolar wire patch antenna' concept," *Proc. 2nd Eur. Conf. Antennas and Propagation (EuCAP)*, 2007.
19. Garg, R., P. Bhartia, I. Bahl, and A. Ittipiboon, *Microstrip Antenna Design Handbook*, Ch. 5, 320, Artech House, Norwood, MA, 2001.